

# Decoding the quark-gluon plasma with jet quenching observables

**Konrad Tywoniuk**

Departament d'Estructura i Constituents de la Matèria and Institut de Ciències del Cosmos (IC-CUB),

Universitat de Barcelona, Martí i Franquès 1, 08028 Barcelona, Spain

E-mail: [konrad@ecm.ub.edu](mailto:konrad@ecm.ub.edu)

**Abstract.** We briefly describe two interesting aspects of heavy-ion collisions related to jets and medium dynamics. First, we discuss how the interaction with the medium change the energy and internal distributions of a QCD jet. Secondly, we discuss a possible manifestation of effects from the confining (chromo)magnetic scale for quark excitations in a realistic plasma.

## 1. Jet modifications in heavy-ion collisions

Jets emerging from heavy-ion collisions are unique probes of the underlying dynamics [1]. Being multi-particle configurations, their detailed substructure is very sensitive to interactions with the dynamical medium, characterised by the transport coefficient  $\hat{q}$ , in course of the branching process. The complexity of the resulting multi-scale evolution is reduced by the presence of a hard scale, related to the jet energy and opening angle  $Q = E\Theta_{\text{jet}}$ , which is much larger than any characteristic momentum scale of the medium, see below [2]. This scale separation guarantees the validity of a perturbative framework. Since any coloured high-energy particle propagating through the medium (color current) perturbs the background field and leads to stimulated radiation, former studies mainly addressed the jet modifications in medium arising from induced radiation [3]. The dynamical interplay of jet and medium scales in course of the evolution is, however, to a large extent unknown, although models based on perturbative arguments exist [4].

The problem has been worked out in detail on the level of a time-like single emission off a dipole [5, 6]. It was shown that the decoherence of the dipole is governed by the “decoherence parameter,” defined as  $\Delta_{\text{med}} = 1 - \exp[-(r_{\perp}Q_s)^2/12]$ , which marks out two characteristic medium scales with simple geometric interpretations. On the one hand,  $r_{\perp} = \theta_0 L$  is the transverse size of a dipole with opening angle  $\theta_0$  traversing a medium of length  $L$ . On the other hand,  $Q_s = \sqrt{\hat{q}L}$  determines the accumulated transverse momentum (via Brownian motion) of a probe passing through a medium characterized by the diffusion coefficient  $\hat{q}$ . Whenever the dipole is small enough, such that  $r_{\perp}^{-1} \gg Q_s$ , the decoherence parameter is vanishing. This means that the medium only resolves the total charge of the dipole. In this case, it is also the total charge that gives rise to medium-induced radiation. In the opposite case, whenever the medium scale is large,  $r_{\perp}^{-1} \ll Q_s$ , the individual charges of the dipole are resolved and can induce radiation.

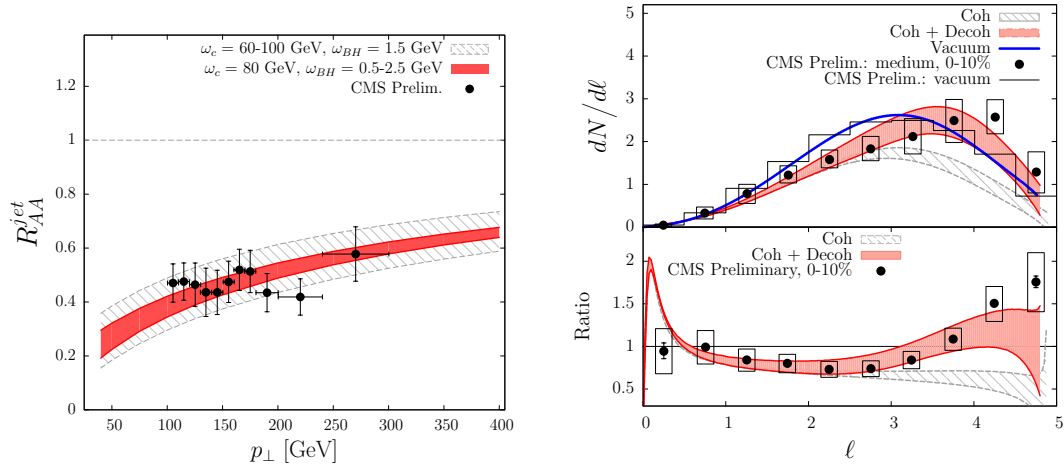


**Figure 1.** Left panel: The nuclear modification factor calculated with  $\omega_c = 80$  GeV as a function of jet  $p_{\perp}$  for central Pb-Pb collisions. The dark (red) band includes the variation of  $\omega_{BH}$  around a central value of 1.5 GeV. The light (grey) band includes, in addition, a variation of  $\omega_c \in [60, 100]$  GeV. The experimental data are taken from [13]. Right, upper panel: the longitudinal fragmentation function plotted as a function of  $\ell = \ln 1/x$ . Right, lower panel: the ratio of medium-modified and vacuum fragmentation functions for a jet with  $E = 100$  GeV and  $\Theta_{\text{jet}} = 0.3$ . The experimental data are taken from [14]. The figures in both panels are taken from [12].

We therefore can think of the jet-medium interaction in a twofold way [2]. The interplay of scales at each step of the fragmentation determines simultaneously the number of independent (or color decoherent) sources of medium-induced radiation as well as the phase space for soft and collinear emissions [7, 8, 9]. The former process is crucial in redistributing the jet energy up to very large angles, mostly far out of the jet cone [10]. The latter modifies the familiar angular ordering features [11] and brings about modifications to the inter-jet distribution, mostly within the cone.

For a sample of the jets with the highest energy available in heavy-ion collision reconstructed at relatively small cone sizes, we expect to be dominated by collimated jets, i.e. situations where the major fraction of the jet energy is located close to the jet axis [2]. When calculating inclusive observables, such as the jet spectrum, one can therefore treat the whole jet as coherent system, interacting with the medium as a whole [12]. The inter-jet observables, e.g. the energy distribution of final-state hadrons in the jet, are however more sensitive to the effects of decoherence which can strongly alter the yield of soft particles inside the cone.

First let us address the modification to the inclusive jet spectrum, typically quantified through the nuclear modification factor defined as  $R_{AA}^{\text{jet}} \equiv d^2 N_{\text{Pb-Pb}}^{\text{jet}}(p_{\perp})/d^2 p_{\perp} / (T_{AA} d^2 \sigma_{\text{p-p}}^{\text{jet}}(p_{\perp})/d^2 p_{\perp})$ , where  $T_{AA}$  is the nuclear overlap function. Thus, the spectrum after passing through the medium is computed by convoluting the jet cross-section in vacuum, proportional to the quark cross-section, with the distribution of quarks,  $D_q^{\text{med}}$ , after passing through the medium. The distribution  $D_q^{\text{med}}$  was found from the rate equation described above with the parameters  $\alpha_s = 0.5$  and an energy cut-off  $\omega_{BH} = 1.5$  GeV [12]. The central value obtained from the left panel in Fig. 1 results in  $\omega_c \equiv Q_s^2 L/2 = 80$  GeV. To gauge the uncertainties related to the choice of our parameters, we have also allowed the medium parameters to vary giving rise to the shaded region in Fig. 1. To establish a closed set of physical energy and momentum scales,

we have also chosen  $L = 2.5$  fm resulting in the medium scale  $Q_s = 3.6$  GeV, and  $Q_s \ll Q$  as expected. This naturally leads to a small deflection of the jet while 14–19% of the energy flows out a cone of  $\Theta_{\text{jet}} = 0.3$  which agrees qualitatively with experimental measurements [15].

The modifications of the fragmentation functions of jets are more subtle. We will focus on the so called intra-jet energy distribution of hadrons  $dN^{\text{vac}}/d\ln(1/x) \equiv D^{\text{vac}}(x; Q)$  which is typically plotted in terms of the variable  $\ell = \ln(1/x_h)$  where  $x$  is fraction of the jet energy carried by the parton. The  $Q$  dependence of  $D^{\text{vac}}$  is governed by the MLLA evolution equations [11] which obey angular ordering. The thin, solid (grey) lines in the right panel of Fig. (1) represent the energy distribution within a completely coherent jet with reduced energy and fails to describe the data. The thick, solid (red) curves demonstrate the effect of decoherence, which plays a crucial role only for soft gluons. The bands represent uncertainties in the jet ( $\sim 20\%$ ) and medium scales. See [12] for further details.

## 2. Novel excitations of hot quarks

In recent years, there has been compelling evidence that a strongly coupled system is created in ultrarelativistic heavy-ion collisions. We are tempted to ask: what are the fundamental degrees of freedom of such a system? And how can we use external probes, e.g. such as jets, to precisely pin down these features? The underlying dynamics is governed by QCD, the theory of strong interactions, but a perturbative expansion in the ordinary setup is tractable only for asymptotically large temperatures. There are nevertheless strong indications that a confinement mechanism has to be incorporated within perturbative resummation even when dealing with the QGP phase.

When addressing these questions, one has to take the problem of quantizing the theory seriously. A formalism to tackle this issue is the Gribov-Zwanziger (GZ) action, which is well known from studies of color confinement [16, 17]. In general covariant gauges, the ghost and gluon propagators are modified. Additionally, a new scale, the Gribov parameter  $\gamma_G$ , is generated from the fixing of the infrared residue gauge transformations after the Faddeev-Popov procedure. This scale is determined by a self-consistent gap equation, which at one-loop order gives  $\gamma_G = \frac{3N_c}{16\sqrt{2}\pi}g^2T$  at asymptotically high temperatures, where  $N_c$  is the number of colors [18, 19]. The Gribov parameter provides a fundamental infrared cutoff at the confining (chromo)magnetic scale for the GZ action and the resulting equations of state show stable and robust behavior that is consistent with lattice data down to nearly the deconfinement transition [19]. These results therefore highlight the significant role played by the magnetic scale in the phenomenologically relevant temperature regime.

In order to get a handle on what the relevant degrees of freedom are, we have recently studied the quasi-particle quark excitations of a finite temperature QCD plasma [20] using systematics of the hard-thermal-loop (HTL) effective theory [21]. Our results are plotted in Fig. 2 for a relevant range of couplings  $g \lesssim 2$ . As expected, we recover the screened quasi-particle  $\omega = \omega_+(p; \gamma_G)$  and hole  $\omega = \omega_-(p; \gamma_G)$  excitations of the plasma, depicted by dashed-dotted and dashed (blue) curves in Fig. 2. The low-momentum limit of dispersion relation corresponds to the screening mass,  $\omega_{\pm}(0; \gamma_G) = m_q(\gamma_G)$ , which in our calculation incorporates effects from the magnetic scale and reduces to the well know fermionic Debye mass,  $m_q(0) = \sqrt{C_F/8}gT$ .

In stark contrast to the conventional HTL expectation, we also find a third pole in the quark propagator with  $\omega = \omega_G(\omega; \gamma_G)$ . It describes massless fermionic excitations in the plasma which are governed by the dispersion relation  $\omega = v_s p$  at small momenta, see solid (red) curves in Fig. 2. We have numerically established that  $v_s \approx 1/\sqrt{3}$  (speed of sound) independent of the coupling for the studied range. Due to its masslessness, the new mode incorporate long-range correlations of the quark-gluon plasma rendering it strongly correlated. The range in momentum where this pole can exist scales with the magnetic scale through  $\gamma_G$ , and we have plotted it in Fig. 2 for two values of the coupling. Moreover, the pole goes along with a negative weight to

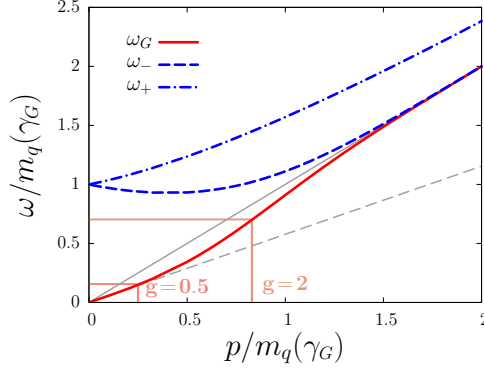


**Figure 2.** Dispersion relations (upper panel) and the corresponding residues (lower panel) for the plasmino ( $\omega_+$ ), anti-plasmino ( $\omega_-$ ) and Gribov ( $\omega_G$ ) poles. The scaling with  $m_q(\gamma_G)$  has been numerically established for  $g \lesssim 2$ . Figure taken from [20].

the spectral function which signals effects of confinement [22], see [20] for a further discussion. It therefore does not represent a physical quark excitation but should rather be a resonance-like mode.

We conclude that these novel features, where the magnetic scale plays a prominent role, are characteristic of the non-Abelian nature of QCD. Their manifestation emphasizes the importance of the long-range confinement effects surviving at finite temperatures in the plasma and will play a crucial role for phenomenology in a realistic range of temperatures.

**Acknowledgements.** The author would like to thank Y. Mehtar-Tani and N. Su for fruitful collaboration. The author is supported by a Juan de la Cierva fellowship and by the research grants FPA2010-20807, 2009SGR502 and by the Consolider CPAN project and by FEDER.

## References

- [1] Mehtar-Tani Y, Milhano J G and Tywoniuk K 2013 *Int.J.Mod.Phys.* **A28** 1340013 (*Preprint* 1302.2579)
- [2] Casalderrey-Solana J, Mehtar-Tani Y, Salgado C A and Tywoniuk K 2013 *Phys.Lett.* **B725** 357–360 (*Preprint* 1210.7765)
- [3] Salgado C A and Wiedemann U A 2002 *Phys.Rev.Lett.* **89** 092303 (*Preprint* hep-ph/0204221)
- [4] Zapp K, Ingelman G, Rathsman J, Stachel J and Wiedemann U A 2009 *Eur.Phys.J.* **C60** 617–632 (*Preprint* 0804.3568)
- [5] Mehtar-Tani Y, Salgado C and Tywoniuk K 2012 *Phys.Lett.* **B707** 156–159 (*Preprint* 1102.4317)
- [6] Casalderrey-Solana J and Iancu E 2011 *JHEP* **1108** 015 (*Preprint* 1105.1760)
- [7] Mehtar-Tani Y, Salgado C A and Tywoniuk K 2011 *Phys.Rev.Lett.* **106** 122002 (*Preprint* 1009.2965)
- [8] Mehtar-Tani Y and Tywoniuk K 2013 *JHEP* **1301** 031 (*Preprint* 1105.1346)
- [9] Mehtar-Tani Y, Salgado C A and Tywoniuk K 2012 *JHEP* **1210** 197 (*Preprint* 1205.5739)
- [10] Blaizot J P, Fister L and Mehtar-Tani Y 2014 (*Preprint* 1409.6202)
- [11] Khoze V A and Ochs W 1997 *Int.J.Mod.Phys.* **A12** 2949–3120 (*Preprint* hep-ph/9701421)
- [12] Mehtar-Tani Y and Tywoniuk K 2014 (*Preprint* 1401.8293)
- [13] CMS Collaboration 2012 (*Preprint* CMS-PAS-HIN-12-004)
- [14] CMS Collaboration 2012 (*Preprint* CMS-PAS-HIN-12-013)
- [15] Chatrchyan S *et al.* (CMS Collaboration) 2011 *Phys.Rev.* **C84** 024906 (*Preprint* 1102.1957)
- [16] Gribov V 1978 *Nucl.Phys.* **B139** 1
- [17] Zwanziger D 1989 *Nucl.Phys.* **B323** 513–544
- [18] Zwanziger D 2007 *Phys.Rev.* **D76** 125014 (*Preprint* hep-ph/0610021)
- [19] Fukushima K and Su N 2013 *Phys.Rev.* **D88** 076008 (*Preprint* 1304.8004)
- [20] Su N and Tywoniuk K 2014 (*Preprint* 1409.3203)
- [21] Braaten E and Pisarski R D 1990 *Nucl.Phys.* **B337** 569
- [22] Alkofer R and von Smekal L 2001 *Phys.Rept.* **353** 281 (*Preprint* hep-ph/0007355)